Parametric Instability Boundaries for Spatial Subharmonics in Photorefractive Moving Gratings: Theory and Experiments

Chong Hoon Kwak and El-Hang Lee

CONTENTS

ABSTRACT

We have derived a nonlinear spatio-temporal differential equation for space-charge fields from Kukhtarev's material equations in a moving coordinate system and obtained the spatial subharmonic instability boundaries by using linear stability analysis. It is also found that there is an analogy between the temporal subharmonic and the spatial subharmonc instabilities in the sense that the governing differential equations describing the instability boundaries are formally identical. The experiments for generating spatial subharmonic waves are performed in a photorefractive $Bi_{12}SiO_{20}$ crystal by using conventional moving grating technique. The threshold detunings are experimentally determined and the results are compared with the theory.

I. INTRODUCTION

The interaction of optical waves in photorefractive materials has been intensively studied over the past two decades [1]-[3]. Photorefractive materials are one of the most versatile materials for use in optical signal processing. They can be used in a wide range of applications because photorefractive media provide unique features like real time operation, high optical gain, data storage, nonlinear operation and correlation. These include [1], [4]: real time holography, image amplification, laser beam steering, vibrational analysis, laser gyros, nonreciprocal transmission, neural network, parallel half-adder circuit, optical correlator, novelty filter, pattern recognition, dynamic optical interconnections and photonic switching. The basic building block for these versatile applications is two-wave mixing geometry.

In 1988, Mallick *et al.* [5] observed spatial subharmonic waves by illuminating photorefractive $Bi_{12}SiO_{20}$ crystal with two coherent beams of equal intensities and by detuning one of the pump beams and applying external dc electric field on the crystal (*i.e.*, by moving grating technique). Since the first generation of spatial subharmonics in a two-wave mixing geometry, there have been further observations of subharmonics [6]-[16] as well as various attempts to provide theoretical explanations [7], [9], [12]-[20]. In experimental sides, there have been further developments for generation of spatial subharmonics by applying ac electric field instead of the moving grating technique [10], [13], [16] and using different materials such as $Bi_{12}TiO_{20}$ [11] and $Bi_{12}GeO_{20}$ [14].

The theories developed up to now could be divided into three classes: the first being based on the interactions between the beams [7], the second, on the spontaneous growth of the subharmonics [9], [10], [12]-[14], [17]-[19], and the third, on the combined effect of the above two mechanisms [20]. In mathematical terms, the first method is based on the field equations, describing the way that the waves are coupled to each other in the presence of a subharmonic grating *a priori* as well as a fundamental grating, whereas the second one is regarded as an instability analysis of the material equations against period doubling, and the last one takes into account the field equations and material equations simultaneously. Both sets of differential equations are nonlinear and were proposed in a paper by Kukhtarev *et al.* [2].

Before we embark on a detailed analysis of the spatial subharmonic instability, it may be interesting to compare the corresponding temporal subharmonic instability with the spatial one. It is well-known [21] that a tuned RLC circuit (resistance, inductor and capacitor in series) where the capacitance is made to vary at a frequency Ω will contain an $\Omega/2$ term in its frequency response (Fig.1). The corresponding temporal differential equation is then given by

$$\ddot{Q} - \kappa\dot{Q} + (a + g\cos\Omega t)\,Q = 0 \qquad (1)$$

where the dot represents the time derivative, Q is the electric charge and the coefficients depend on the values of the various circuit

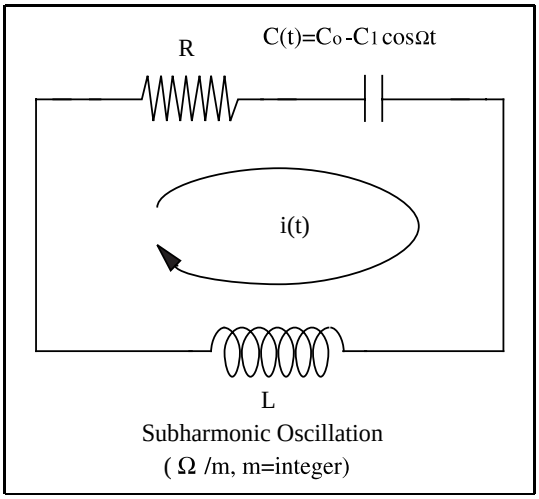

Fig. 1. Nonlinear RLC circuit generating temporal subharmonic oscillation.

elements. This is known as damped Mathieu equation which has a region of instability against period doubling (*i.e.*, an unstable region occurring $\Omega/2$ subharmonic oscillation) when

$$\frac{1}{4}-\frac{1}{2}\sqrt{g^2-\kappa^2}\le a\le\frac{1}{4}+\frac{1}{2}\sqrt{g^2-\kappa^2}. \qquad (2)$$

In this paper, we investigate the physical origin of the subharmonic instability both theoretically and experimentally. First, in Sec. II, for analytic descriptions of the spatial subharmonics, we derive a nonlinear differential equation for the space-charge field from material equations in a moving coordinate system, which reduces to the damped Mathieu equation for steady state. In Sec. III, we examine the stability criteria for the spatial subharmonic solution of the nonlinear differential equation derived in Sec. II by using linear stability ana-lysis and obtain the parametric instability boundaries. We, furthermore, identify the spatial subharmonic oscillations with a classical damped harmonic oscillator in Sec. IV and classify the stability solutions of the spatial subharmonics by examining the characteristic roots of the solutions. Finally, in Sec.V, the threshold detuning conditions for instability curves are experimentally determined and the results are compared with the theory.

II. SUBHARMONIC SPACE-CHARGE FIELD IN A MOVING COORDINATE SYSTEM

In this section we derive the nonlinear partial differential equation for the space-charge field describing the spatial subharmonics from material equations [2]:

$$\frac{\partial N_D^+}{\partial t}=(sI+\beta)(N_D-N_D^+)-\gamma_R n N_D^+, \qquad (3)$$

$$e\frac{\partial N_D^+}{\partial t}=e\frac{\partial n}{\partial t}-\frac{\partial J}{\partial x}, \qquad (4)$$

$$\frac{\partial E}{\partial x}=\frac{e}{\varepsilon_o\varepsilon_s}(N_D^+-N_A-n), \qquad (5)$$

$$J=e\mu nE+k_BT\mu\frac{\partial n}{\partial x}, \qquad (6)$$

where N_D^+ and N_D are the ionized donor density and donor density, respectively, N_A the acceptor density, n the electron density, J the current density, E the electric field, I the light intensity, s the cross section of photoionization, β the thermal generation rate, γ_R the recombination constant, ε_o the free space permittivity, ε_s the relative static dielectric constant, μ the mobility, e the electron charge, k_B the Boltz-

mann constant and T the temperature. For simplicity, we introduce some simplifications as used in [3], into the above material equations: (i) $n \ll N_D^+$, (ii) $N_D^+ \ll N_D$, (iii) $\beta \ll sI$ and (iv) ε_s is independent of x and (v) there is no diffusion effect in the current density J.

When the intensity interference fringes are formed by two plane pump beams with the propagating wave vectors $\mathbf{K}_1$ and $\mathbf{K}_2$ as illustrated in Fig. 2, the intensity distribution illuminating a photorefractive material is given by $I(x,t) = I_o[1 + m\cos(Kx - \Omega t)]$ where I_o is the average intensity, m is the modulation, $\mathbf{K} = \mathbf{K}_1 - \mathbf{K}_2$ is the fundamental spatial frequency (fundamental grating wave vector), K is the magnitude of $\mathbf{K}$ and Ω is the detuning frequency of one of the two pump beams. Figure 2 depicts the schematic diagram for the diffracted waves including subharmonics and super-subharmonics as well as higher harmonic waves generated in a photorefractive moving grating. We now introduce a moving coordinate system of the variables,

$$\xi = Kx - \Omega t, \text{ and } t_d = sI_o t \tag{7}$$

and assume that all the physical variables used in (3) to (6) vary in the same periodic manner with ξ and take a solution of the form:

$$Y(\xi, t_d) = Y_o + Y_1(\xi, t_d), \tag{8}$$

where Y_i $(i = 0, 1)$ stand for the physical variables such as N_D^+, n, J and E. Here, Y_o is spatially uniform part and is independent of time and $Y_1(\xi, t_d)$ is spatially modulated part. It is noted that although the driving source yielding all the grating diffraction comes from the moving intensity interference pattern, $I_1 = mI_o\cos\xi$, the modulation $Y_1(\xi, t_d)$ is not linearly propotional to I_1 any more because of quadratic recombination of n and N_D^+ as in (3). Using the transformation relations of the form,

$$\frac{\partial}{\partial x} = K\frac{\partial}{\partial \xi}, \text{ and } \frac{\partial}{\partial t} = -\Omega\frac{\partial}{\partial \xi} + sI_o\frac{\partial}{\partial t_d}, \tag{9}$$

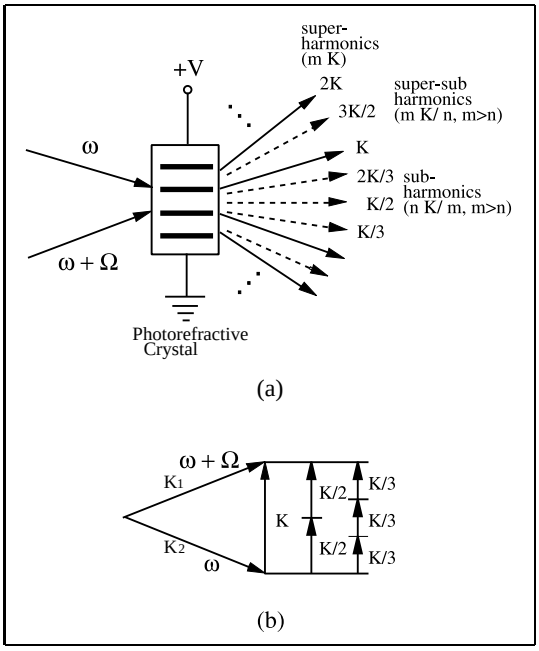

Fig. 2. Schematic diagram for fundamental grating (K) and spatial subharmonic gratings $(nK/m,\ m > n$ and $m, n =$integer) as well as super-subharmonics $(mK/n, m > n)$ in a photorefractive moving grating. Ω is a detuning frequency of one of the pump beams. Only a few of subharmonic grating wave vectors (K/m) are presented in (b), for simplicity.

and then substituting (7) and (9) into (3) through (6) and separating the subscripts 0 and

1, we have the following equations for the subscript 0 (*i.e.*, for spatially uniform terms):

$$N_{D_0}^{+} = N_A, \tag{10a}$$

$$n_0 = \frac{sI_0 N_D}{\gamma_R N_A}, \tag{10b}$$

$$J_0 = e\mu n_0 E_0 \tag{10c}$$

and for the subcript 1 (*i.e.*, for spatially nonuniform terms):

$$\begin{aligned} &-\Omega\frac{\partial}{\partial\xi}N_{D1}^{+} + sI_o\frac{\partial}{\partial t_d}N_{D1}^{+} \\ &= sI_1 N_D - \gamma_R n_1 N_A - \gamma_R(n_0+n_1)N_{D1}^{+} \end{aligned} \tag{11a}$$

$$\begin{aligned} &-\Omega\frac{\partial}{\partial\xi}N_{D1}^{+} + sI_o\frac{\partial}{\partial t_d}N_{D1}^{+} \\ &= -\mu K\frac{\partial}{\partial\xi}(n_0E_1 + n_1E_0 + n_1E_1) \end{aligned} \tag{11b}$$

$$\frac{\partial}{\partial\xi}E_1 = \frac{e}{\varepsilon_0\varepsilon_s K}N_{D1}^{+}. \tag{11c}$$

Substituting (11c) into (11a), we get

$$\begin{aligned} &-\Omega\frac{\partial^2}{\partial\xi^2}E_1 + sI_0\frac{\partial^2}{\partial\xi\partial t_d}E_1 \\ &= \frac{e}{\varepsilon_0\varepsilon_s K}sI_1N_D - \frac{e}{\varepsilon_o\varepsilon_s K}\gamma_R n_1 N_A \\ &-\gamma_R(n_0+n_1)\frac{\partial}{\partial\xi}E_1 \end{aligned} \tag{12}$$

where $I_1 = mI_0\cos\xi$. Substituting now (11c) into (11b) and then integrating it with respect to ξ, it becomes

$$\begin{aligned} &-\Omega\frac{\partial}{\partial\xi}E_1 + sI_0\frac{\partial}{\partial t_d}E_1 \\ &= -\frac{e\mu}{\varepsilon_0\varepsilon_s}(n_0E_1 + n_1E_0 + n_1E_1) + C(t_d) \end{aligned} \tag{13}$$

where $C(t_d)$ is an integration constant and is independent of ξ. Here, we take the integration constant to be zero without loss of generality. Eliminating n_1 from (12) and (13), and rearranging the terms, finally we obtain the following nonlinear partial differential equation for the varying part of the space charge field $E_1(\xi, t_d)$:

$$\begin{aligned} &\left[-\Omega\frac{\partial^2}{\partial\xi^2}E_1 + sI_0\frac{\partial^2}{\partial\xi\partial t_d}E_1\right. \\ &\left. + \frac{1}{\tau_d}\frac{E_M}{E_q}\frac{\partial}{\partial\xi}E_1 - \frac{E_M}{\tau_d}m\cos\xi\right](E_0+E_1) \\ &= \left[-\Omega\frac{\partial}{\partial\xi}E_1 + sI_0\frac{\partial}{\partial t_d}E_1 + \frac{1}{\tau_d}E_1\right] \\ &\quad\times\left(E_M + \frac{E_M}{E_q}\frac{\partial}{\partial\xi}E_1\right) \end{aligned} \tag{14}$$

where E_0 is applied field, $E_q = \dfrac{eN_A}{\varepsilon_0\varepsilon_s K}$, $E_M = \dfrac{\gamma_R N_A}{\mu K}$ and $\tau_d = \dfrac{\varepsilon_0\varepsilon_s}{e\mu n_0}$. Equation (14) is a most general spatio-temporal differential equation describing all the diffraction phenomena including subharmonics as well as fundamental grating occuring in photorefractive materials. It is readily to show that if we take a solution of the fundamental space-charge field as $E_1(\xi, t_d) = A_1(t_d)\exp[i\xi] + c.c.$ and substitute into (14), after simple calculations, $A_1(t_d)$ reduces to the well-known form of fundamental space-charge field for moving grating [3]. For steady state case (*i.e.*, $\dfrac{\partial}{\partial t_d} \to 0$), (14) becomes

$$\left(1+\frac{E_1}{E_0}\right)\frac{\partial^2}{\partial\xi^2}E_1 - \left(\frac{E_M}{bE_q} + \frac{E_M}{E_0}\right)\frac{\partial}{\partial\xi}E_1$$

$$+\frac{E_M}{bE_0}(1+m\cos\xi)E_1 = \\ =-\frac{E_M}{b}m\cos\xi+\frac{E_M}{E_0E_q}\left(\frac{\partial}{\partial\xi}E_1\right)^2, \tag{15}$$

where $b=\Omega\tau_d$ is a dimensionless detuning frequency. It is noted that (15) is formally identical to the damped Mathieu equation, (1), for a tuned RLC circuit except for additional driving and nonlinear terms in the right hand side.

III. LINEAR STABILITY ANALYSIS FOR SPATIAL SUBHARMONICS

In order to examine the stability for $K/2$-spatial subharmonic solution of (14), we take a solution of the form

$$E_1(\xi,t_d) \\ =A^+(t_d)\exp\left[\frac{i}{2}\xi\right]+A^-(t_d)\exp\left[-\frac{i}{2}\xi\right] \tag{16}$$

where $A^{\pm}(t_d)$ represent the amplitudes of forward and backward propagating subharmonic space-charge fields in ξ-axis, respectively. For simplicity, we neglect the fundamental space-charge field and higher (sub and/or super) harmonic terms in a solution form of (16). On substituting (16) into (14) and equating terms with the same exponential dependence, we get a set of coupled wave equations:

$$\left(\frac{i}{2}E_0-E_M\right)sI_0\frac{\partial A^+}{\partial t_d} \\ +\left(\frac{\Omega}{4}E_0-\frac{E_M}{\tau_d}+\frac{i}{2}\Omega E_M\right)A^+ \\ =\frac{mE_M}{2\tau_d}A^-, \tag{17a}$$

$$\left(\frac{i}{2}E_0+E_M\right)sI_0\frac{\partial A^-}{\partial t_d} \\ -\left(\frac{\Omega}{4}E_0-\frac{E_M}{\tau_d}-\frac{i}{2}\Omega E_M\right)A^- \\ =-\frac{mE_M}{2\tau_d}A^+. \tag{17b}$$

In deriving (17) it is assumed that $E_q \gg E_o > E_M$, which is valid for our experimental condition as will be seen later. By ansatz we take the amplitudes of the form

$$A^{\pm}(t_d)=A_0^{\pm}\exp\left[\lambda\frac{t_d}{sI_0\tau_d}\right], \tag{18}$$

where the parameter λ is the growth or decay rate of the solution according to λ values. Roughly speaking, the amplitudes of (18) are stable if $\mathrm{Re}\{\lambda\}<0$ and unstable if $\mathrm{Re}\{\lambda\}>0$. More detailed characteristics of these stabilities will be discussed in the next section. On substituting (18) into (17), and after some algebra, we obtain the determinant for a nontrivial solution of (17):

$$\begin{vmatrix} a_{11}+ib_{11} & a_{12}+ib_{12} \\ a_{21}+ib_{21} & a_{22}+ib_{22} \end{vmatrix}=0, \tag{19}$$

where

$$a_{11}=\frac{b}{4}E_0-E_M-\lambda E_M, \\ b_{11}=\frac{b}{2}E_M+\frac{\lambda}{2}E_0, \\ a_{12}=-\frac{m}{2}E_M, \\ b_{12}=0$$

and $a_{22} = -a_{11}$, $b_{22} = b_{11}$, $a_{21} = -a_{12}$ and $b_{21} = b_{12} = 0$. Here, $b = \Omega\tau_d$ is the dimensionless quantity that is proportional to the detuning frequency Ω and is inversely proportional to the input intensity. Equation (19) immediately leads to the following characteristic equation for λ:

$$C_0\lambda^2 + C_1\lambda + C_2 = 0, \tag{20}$$

where

$$C_0 = E_M^2 + \frac{E_0^2}{4},$$
$$C_1 = 2E_M^2,$$
$$C_2 = \left(\frac{b}{4}E_0 - E_M\right)^2 + \frac{b^2 - m^2}{4}E_M^2.$$

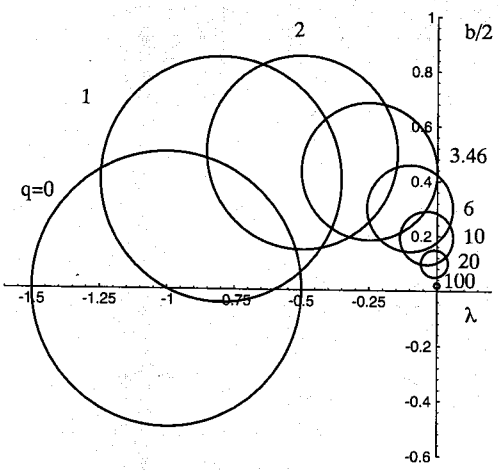

Fig. 3. Parametric circles in complex plane for $m = 1$. For $\lambda < 0$ regions, there is no subharmonic instability. The critical value of q for subharmonic instability is approximately 3.46.

In order to find the conditions when $\mathrm{Re}\{\lambda\} > 0$ or $\mathrm{Re}\{\lambda\} < 0$, first we analyze the characteristic equation, (20), graphically in $(\lambda, b/2)$-plane. It may be readily shown that for each values of $q = E_o/E_M$, the characteristic equation depicts the circle centered at $(-1/(1+q^2/4), q/[2(1+q^2/4)])$ with the radius of $m^2/[4(1+q^2/4)]$ as shown in Fig. 3. The two crossing points with the $b/2$-axis at $\lambda = 0$ give the threshold values of b for subharmonic instabilities. The minimum condition for subharmonic instability is approximately given by $q \geq 3.46$ (*i.e.*, $E_{o,\min} \geq 3.46E_M$), which will be later confirmed analytically. For $q > 3.46$, there are positive λ regions on each circles.

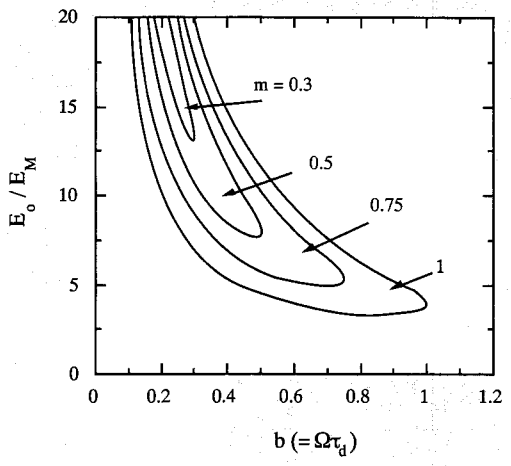

Fig. 4. Threshold subharmonic instability regions for various modulation m. Spatial subharmonic waves exist inside the banana curves for each modulation m.

Now, in order to seek the instability boundaries of the system analytically, one may apply the Hurwitz criterion to the characteristic equation. It follows from the Hurwitz criterion that (18) is stable if $C_0 > 0$, $C_1 > 0$ and $C_1C_2 > 0$

(*i.e.*, when all of the roots of (20) have negative real parts), which, upon substituting the coefficients of (20), leads to

$$\frac{E_0}{E_M} > \frac{4+2\sqrt{m^2-b^2}}{b} \tag{21a}$$

and

$$\frac{E_0}{E_M} < \frac{4-2\sqrt{m^2-b^2}}{b}. \tag{21b}$$

Therefore, we have the boundaries of the instability regions for the spatial subharmonics as

$$\frac{E_0}{E_M} = \frac{4\pm 2\sqrt{m^2-b^2}}{b}. \tag{22}$$

It may be noted that the expression for the instability boundaries from (22) is the same as that obtained from damped Mathieu equation (see (2)). Figure 4 represents the spatial subharmonic instability regions for several values of the modulation index m. From (22) the minima of the boundary curves and the corresponding values of detuning are given by

$$\left(\frac{E_0}{E_M}\right)_{\text{min.}} = \frac{4}{m}\sqrt{1-\frac{m^2}{4}} \tag{23a}$$

and

$$b_{\text{min.}} = m\sqrt{1-\frac{m^2}{4}}. \tag{23b}$$

IV. CLASSIFICATION OF STABILITY SOLUTIONS FOR SUBHARMONICS

In the preceding section, we found it useful to adapt the linear stability analysis in order to find the subharmonic instability boundary conditions. In this section, we describe the characteristics of the stability solutions in the phase plane. Eliminating $A^-(t_d)$ from (17) and putting $x(t_d) = A^+(t_d)$ we have the equation of motion for spatial subharmonic oscillator in photorefractive materials:

$$\ddot{x} + 2P\dot{x} + \omega_0^2 x = 0, \tag{24}$$

where the dot represents the time derivative. Here,

$$P = \frac{1}{\tau_d s I_0 \left(1+\frac{q^2}{4}\right)}, \tag{25a}$$

$$\omega_0^2 = \frac{\left[\left(\frac{b}{4}q-1\right)^2 + \frac{b^2-m^2}{4}\right]}{(\tau_d s I_0)^2\left(1+\frac{q^2}{4}\right)} \tag{25b}$$

and

$$q = \frac{E_0}{E_M}, \tag{25c}$$

where P is real and positive. For the singular points (or the equilibrium points), the roots of the characteristic equation of (25) are given by the following expression

$$\lambda = -P \pm \sqrt{P^2-\omega_0^2}. \tag{26}$$

As we shall see later, the nature of the solution $x(t_d)$ is wholly governed by the nature of the characteristic roots λ_1 and λ_2. In general, several types of solutions are possible: stable (unstable) node, stable (unstable) focus, center and saddle point. However, in our physical system, the following three types of singularities can occur:

(i) When $P^2 > \omega_0^2$ and $\omega_0^2 > 0$, *i.e.*, when the roots λ_1 and λ_2 are real and negative, the singularity is a stable node.

(ii) When $\omega_0^2 > P^2$ and $\omega_0^2 > 0$, *i.e.*, when the roots λ_1 and λ_2 are complex and their real part is negative, the singularity is a stable focus.

(iii) When $\omega_0^2 < 0$, *i.e.*, when the roots λ_1 and λ_2 are real and have different signs, the singularity is a saddle point. As we know, a saddle point is unstable.

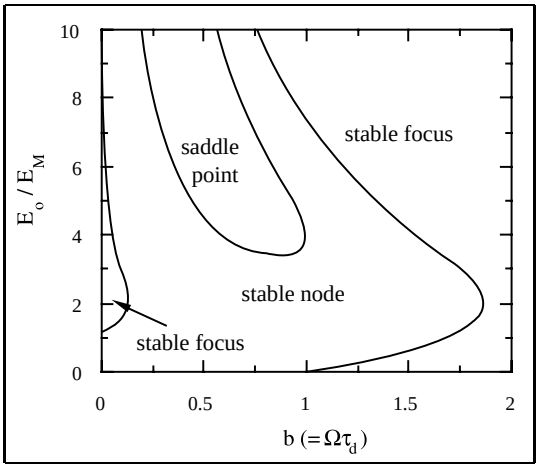

Fig. 5. Phase diagram of stability boundaries for spatial subharmonic oscillator ($m = 1$). The saddle point corresponds to the subharmonic instability region.

The boundary curve between stable node and saddle point is determined by the conditions of (i) and (iii) as $\omega_0^2 = 0$, which leads to the same instability boundaries as from (22). The various kinds of singularities are plotted in Fig. 5 in terms of real physical variables. The saddle point gives the subharmonic instability region. The theoretical prediction for the boundary of the subharmonic instability region describes the experimental result very well as shown in Fig. 7. It is also predicted that if a small perturbation signal is added externally in the same direction of the subharmonic wave it would decay out exponentially in time without oscillation in stable node region and with oscillation in stable focus region (confirming their stability against subharmonics).

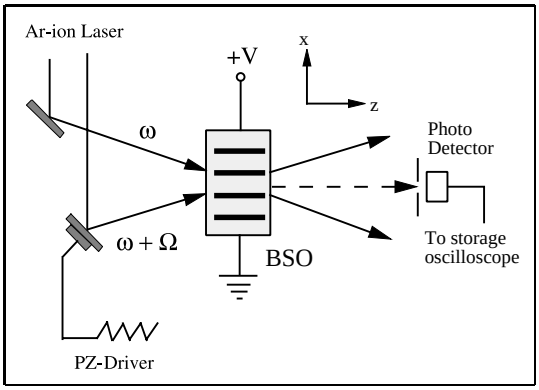

Fig. 6. Schematic diagram of experimental setup for observing spatial subharmonic waves. One of the two incident beams is frequency detuned by a piezoelectric mirror in order to make a moving grating inside the crystal.

V. EXPERIMENTAL RESULTS AND DISCUSSION

The schematic diagram of experimental arrangement for observing the subharmonic waves in photorefractive $Bi_{12}SiO_{20}$ (BSO) crystal is illustrated in Fig. 6. A beam from an Ar-ion laser at a wavelength of 514.5nm is expanded, collimated and split into two beams. The two pump beams which are perpendicularly polarized to the plane of incidence are in-

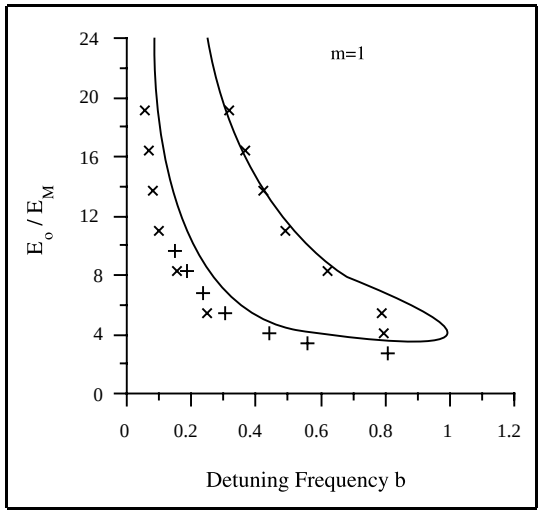

Fig. 7. The instability boundaries of the spatial subharmonics for modulation $m = 1$. The experimental data points $(\times)$ are obtained at the interbeam angle of 2^o and the points $(+)$ at 1^o and the experimental data are taken from [12].

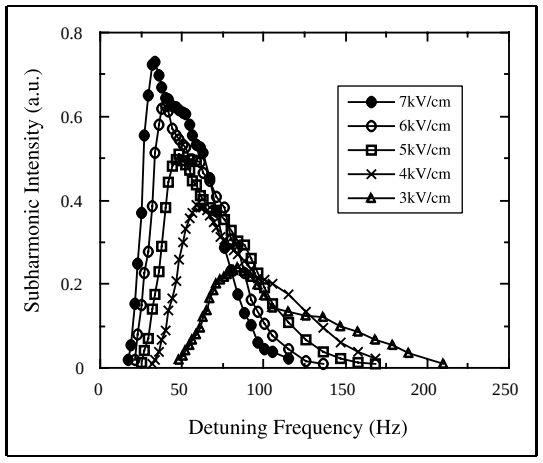

Fig. 8. Measured $K/2$-subharmonic intensity versus detuning frequency for several dc electric fields.

cident on the (110) direction of a BSO crystal grown by Sumitomo ($1 \times 1 \times 1$cm) with antireflection coatings on the input and output surfaces. One of the pump beams is frequency detuned by applying a triangular signal to a piezoelectric mirror as shown in Fig. 6. A dc electric field of up to 7 kV/cm is applied along the (001) direction to the crystal. The two interbeam angles 2° and 1° resulting in the grating spacings of 15 μm ($K = 4.2 \times 10^5 \mathrm{m}^{-1}$) and 30 μm ($K/2 = 2.1 \times 10^5 \mathrm{m}^{-1}$), respectively, are used in the experiments. The total input intensity of 7.6 mW/cm^2 is kept constant during both experimental configurations. The subharmonic intensities are measured by focusing the subharmonic beam with a lens through a small aperture in front of a photodetector, which is connected to a digital storage oscilloscope and a digital multimeter in order to accurately measure the (threshold) subharmonic intensities. Since our main interest in this paper is to investigate the subharmonic instability regions, we measure the detuning frequencies at the lower and upper threshold of the subharmonic waves. Although there is no standard definition for threshold detuning frequencies, we take one at which the subharmonic power is equal to 1.3 times the background noise intensity measured without applied field and with two pump beams. Our criterion for threshold frequency is warranted by the fact that there is a sudden increase of subharmonic intensities above this lower threshold detuning frequency. We also apply this criterion to the upper threshold for the same reason. Figure 7 shows the typical experimental and theoretical curves for threshold subharmonic instability for modulation $m = 1$. The theoretical curves are in good agreement

with the experimental curves. From the best theoretical fit with experiments we have $\tau_d =$ 3.25ms for total input intensity of 7.6 mW/cm^2 and $E_M = 0.365$ kV/cm for $K = 4.2 \times 10^5 \mathrm{m}^{-1}$, which gives us the following crystal parameters; $\gamma_R N_A/\mu = 1.53 \times 10^{10} V\mathrm{m}^{-2}$ and $sN_D = 1.8 \times 10^{20} J^{-1}\mathrm{m}^{-1}$, which is in a reasonable agreement with the literature [3] and [12]. For the experiments at the interbeam angle of 1° (*i.e.*, $K/2 = 2.1 \times 10^5 \mathrm{m}^{-1}$) we have no longer any adjustable parameters. The angle is halved so the value of E_M doubles, and the value of τ_d remains unaffected. It is clearly seen that, as theory predicted, the critical values of the dimensionless detuning frequencies are less than the modulation m for subharmonic instabilities as shown in Figs. 4 and 7. Figure 8 illustrates the measured subharmonic intensity versus detunig frequency for several values of applied electric field. In the measurements, we used total input intensity of 7.6 mW/cm^2, modulation $m = 1$ and grating spacings of 15μm. The detuning curves depict the resonance behavior as the detuning frequency varies. It shows that the subharmonic intensities rapidly increase with an increase of the detuning frequency and then decrease. As the electric field increases, the subharmonic intensity also increases whereas the optimum frequency decreases.

VI. CONCLUSION

We have investigated spatial subharmonics observed in a photorefractive $Bi_{12}SiO_{20}$ crystal under conditions of dc applied electric field and detuning the frequencies of one of the two pump waves. A spatio-temporal differential equation is obtained from the Kukhtarev's material equations in a moving coordinate system and a linear stability analysis is adopted to describe parametric instability regions (*i.e.*, the range of the frequency detuning of the input beams for the spontaneous growth of spatial subharmonics under a dc electric field). It has been found that there is an analogy between the temporal and the spatial subharmonic instabilities in the sense that the governing differential equations (damped Mathieu equation) for instability regions are formally identical to each other. Furthermore, we have classified the natures of the characteristic solutions of the spatial subharmonic space-charge fields. The experimentally determined threshold detuning values show excellent agreement with the theory.

REFERENCES

[1] P. Gunter, J.-P. Huignard eds., *Photorefractive materials and their applications*, vol. I, New York : Springer-Verlag, 1988.

[2] N. V. Kukhtarev, V. B. Markov, S. G. Odulov, M. S. Soskin and V. L. Vinetskii, "Holographic storage in electro-optic crystals. I. Steady state," *Ferroelectrics*, vol. 22 , pp. 949-960, 1979.

[3] Ph. Refregier, L. Solymar, H. Rajbenbach and J.-P. Huignard, "Two beam coupling in photorefractive $Bi_{12}SiO_{20}$ crystals with moving grating: Theory and experiments," *J. Appl. Phys.*, vol. 58, pp. 45-57, 1985.

[4] M. P. Petrov, S. I. Stepanov and A. V. Khomenko,

Photorefractive crystals in coherent optical systems. New York : Springer-Verlag, 1991.

[5] S. Mallick, B. Imbert, H. Ducollet, J. P. Herriau and J.-P. Huignard, "Generation of spatial subharmonics by two-wave mixing in a nonlinear photorefractive medium," *J. Appl. Phys.*, vol. 63, no. 12, pp. 5660- 5663, 1988.

[6] D. J. Webb and L. Solymar, "Observations of spatial subharmonics arising during two-wave mixing in BSO," *Opt. Commun.*, vol. 74, no. 6, pp. 386-388, 1990.

[7] K. H. Ringhofer and L. Solymar, "New gain mechanism for wave amplification in photorefractive materials," *Appl. Phys. Lett.*, vol. 53, no. 12, pp. 1039-1040, 1988.

[8] D. J. Webb, L. B. Au, D. C. Jones and L. Solymar, "Onset of subharmonics by forward wave interactions in BSO," *Appl. Phys. Lett.*, vol. 57, pp. 1602-1605, 1990.

[9] C. H. Kwak, J. Takacs and L. Solymar, "Spatial subharmonic instability in photorefractive $Bi_{12}SiO_{20}$ crystal," *Electron. Lett.*, vol. 28, no. 6, pp. 530-531, 1992.

[10] J. Takacs and L. Solymar, "Subharmonics in $Bi_{12}TiO_{20}$ crystal with an applied ac electric field," *Optics Lett.*, vol. 17, no. 4, pp.247-248, 1992.

[11] J. Takacs, M. Schaub and L. Solymar, "Subharmonics in photorefractive $Bi_{12}TiO_{20}$ crystal," *Optics Commun.*, vol. 91, pp. 252-254, 1992.

[12] C. H. Kwak, J. Takacs and L. Solymar, "Spatial subharmonic instabilities," *Optics Commun.*, vol. 96, no. 4, pp. 278-282, 1993.

[13] C. H. Kwak, M. Shamonin, J. Takacs and L. Solymar, "Spatial subharmonics in photorefractive $Bi_{12}SiO_{20}$ crystal with a square wave applied field," *Appl. Phys. Lett.*, vol. 62, no. 4, pp. 328-330, 1993.

[14] I. Richter, A. Grunnet-Jepsen, J. Takacs and L. Solymar, "An experimental and theoretical study of spatial subharmonics in a photorefractive $Bi_{12}GeO_{20}$ crystal induced by dc field and moving grating technique," *IEEE J. Quantum Electron.*, vol. 30, no. 7, pp.1645-1650, 1994.

[15] H. C. Pedersen and P. M. Johansen, "Observation of angularly tilted subharmonic gratings in photorefractive bismuth silicon oxide," *Optics Lett.*, vol. 19, no. 18, pp.1418-1420, 1994.

[16] A. Grunnet-Jepsen, L. Solymar, and C. H. Kwak, "Effects of subharmonics on two-wave gain in $Bi_{12}SiO_{20}$ under alternating electric fields," *Optics Lett.*, vol. 19, no. 17, pp.1299-1301, 1994.

[17] O. P. Nestiorkin, "Instability of spatial subharmonics under hologram recording in a photorefractive crystal," *Optics Commun.*, vol. 81, pp. 315-320, 1991.

[18] B. I. Sturman, A. Bledowski, J. Otten and K. H. Ringhofer, "Spatial subharmonics in photorefractive crystal," *J. Opt. Soc. Am.*, vol. B9, no. 5, pp. 672-681, 1992.

[19] A. Grunnet-Jepsen, I. Richter, M. Shamonin and L. Solymar, "Subharmonic instabilities on photorefractive crystals for an applied alternating electric field: Theoretical analysis," *J. Opt. Soc. Am.*, vol. B11, no. 1, pp. 132-135, 1994; E. Serrano, M. Carrascosa, F. Agullo-Lopez and L. Solymar, "Subharmonic instability taking into account higher harmonics," *Appl. Phys. Lett.*, vol. 64, no. 5, pp. 658-660, 1994.

[20] C. H. Kwak, S. Shim and E.-H. Lee, "Coupled wave analysis of spatial subharmonics in photorefractive BSO crystal," *Electron. Lett.*, vol. 30, no. 24, pp. 2063-2064, 1994; S. Shim, C. H. Kwak and E.-H. Lee, "Spatial subharmonics in photorefractive moving grating," to be published in *Appl. Phys. Lett.*

[21] P. Hagedorn, *Nonlinear Oscillations*. Oxford : Clarendon Press, 1981.

Chong Hoon Kwak was born in Taegu, Korea on March 10, 1961. He received the B.S. degree in physics from Kyungbook National University in 1983, the M.S. and Ph. D. degrees in physics (applied optics) from KAIST (Korea Advanced Institute of Science and Technology), Seoul in 1985 and 1988, respectively. His dissertation topic was the photoinduced nonlinear optical effect in amorphous chalcogenide glass and its applications to optical image processing under the direction of Professor Sang Soo Lee.

After receiving the Ph. D. degree, he joined ETRI (Electronics & Telecommunications Research Institute) and has been working as a Senior Researcher at the Research Department since 1988. From July 1991 to June 1992, he worked as a Visiting Scientist at the University of Oxford, U. K. within the framework of International Research Coorperation Program between University of Oxford and ETRI.

He has worked on the areas of optical neural networks, free space optical interconnects, free space photonic switchings, volume holography, optical image processing, photorefractive nonlinear optics and nonlinear optical wave propagation in nonlinear medium. He published several dozens of international journal papers.

Dr. Kwak is a member of the Optical Society of America, Optical Society of Korea, Physical Society of Korea and Korean Institute of Telematics and Electronics.

El-Hang (Howard) Lee graduated from Seoul National University with a B.S. degree (summa cum laude) in electrical engineering in 1970, and subsequently received M.S., M.Phil. and Ph.D. degrees in applied physics from Yale University in 1973, 1975 and 1978, respectively. Dr. Lee then spent two years (1979-80) with Princeton University as a Research Fellow, four years (1980-84) with Monsanto Electronic Materials Company as a Research Scientist, and six years (1984-90) with AT&T Bell Laboratories as a Senior Member of Technical Staff. He has taught and lectured at Seoul National University, Chungnam National University and Korea Advanced Institute of Science and Technology, including Yale and Princeton. His research interests include solid-state/semiconductor sciences and lightwave/photonic/optoelectronic sciences. He has published over 100 papers in major international and domestic journals and proceedings and has given a dozen invited talks at international conferences worldwide. He has been awarded scholarships, fellowships, and outstanding service award, and is cited in Marquis Who's Who and in American Men and Women of Science. He is a member of the American Physical Society, American Association for the Advancement of Science, Sigma Xi, New York Academy of Sciences, Optical Society of America, Materials Research Society of America, SPIE (Executive Director, Korea), IEEE/LEOS Society (Senior Member and Chairman, Korea Chapter), Korean Physical Society (Fellow), Optical Society of Korea (Fellow and Board Member). He has served many times as chairman or as a member of international and domestic conference/workshop committees, program committees and advisory committees. Dr. Lee is currently serving as Director of Research Department at ETRI.